Polysaccharide-reinforced amyloid fibril hydrogels and aerogels (Supporting Information)

Mattia Usuelli,[a] Till Germerdonk,[a] Yiping Cao,[a,‡] Mohammad Peydayesh,[a] Massimo Bagnani,[a] Stephan Handschin,[b] Gustav Nyström,[a,c] and Raffaele Mezzenga[a,d,*]

1 pH equilibration of the amyloid fibril hydrogels

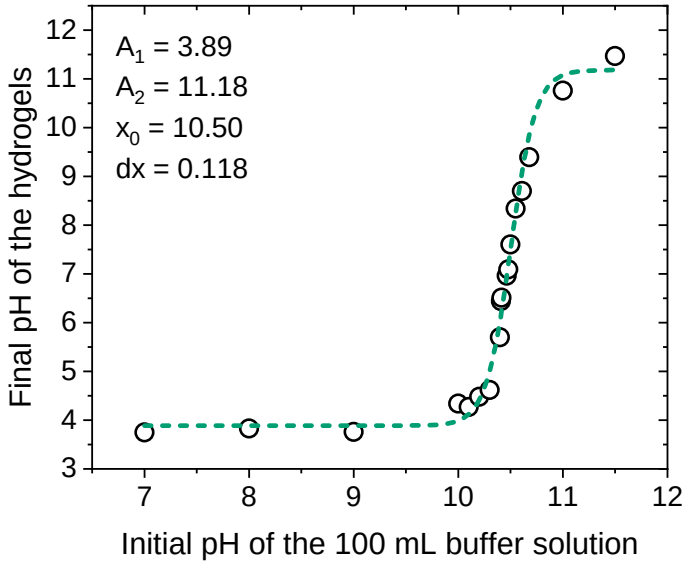

Fig. S1 Equilibration of the pH of the initial βLG hydrogels towards neutral values, by putting 1 mL gels at pH 2 in contact with 100 mL of basic solutions. The decision of using Milli-Q water (adjusted with a concentrated NaOH solution), instead of a more stable buffer system, was made to avoid the presence of salts inside the gel, which could then influence the behaviour of the polysaccharide diffusing units. Before any attempt in fitting the experimental data (black empty circles), it can be appreciated how the pH of the system stays around 4 until the pH of the basic solutions is brought to values larger than 10. The final pH evolves then very steeply as a function of the initial one, encompassing values between 5 and 10 for starting solutions with a pH between 10 and 11; this (expected) behaviour makes a fine adjustment of the final pH delicate, as it is very sensitive to small fluctuations of the initial one. Such sensitiveness was experimentally detected, as we found the final pH of the systems to have a significant standard deviation (up to 2 pH points) from the desired values. The fit of the experimental data is performed with a Boltzmann function ($y = A_2 + (A_1 - A_2)/\exp((x - x_0)/dx)$, green dashed line), that nicely captures the evolution of the data-points (but it would fail at higher pH, as it would saturate instead of following the expected increase of the values).

[a] *ETH Zürich, Department of Health Sciences and Technology, Schmelzbergstrasse 9, 8092 Zürich, Switzerland. E-mail: raffaele.mezzenga@hest.ethz.ch*
[b] *ETH Zürich, Scientific Center for Optical and Electron Microscopy (ScopeM), 8093 Zürich*
[c] *EMPA, Laboratory for Cellulose & Wood Materials, Überlandstrasse 129, 8600 Dübendorf, Switzerland*
[d] *ETH Zürich, Department of Materials, Wolfgang-Pauli-Strasse 10, 8093 Zürich, Switzerland*
‡ Present address: *Department of Chemical Engineering, Massachusetts Institute of Technology, Cambridge, MA 02139, USA*

2 Computation of the persistence length

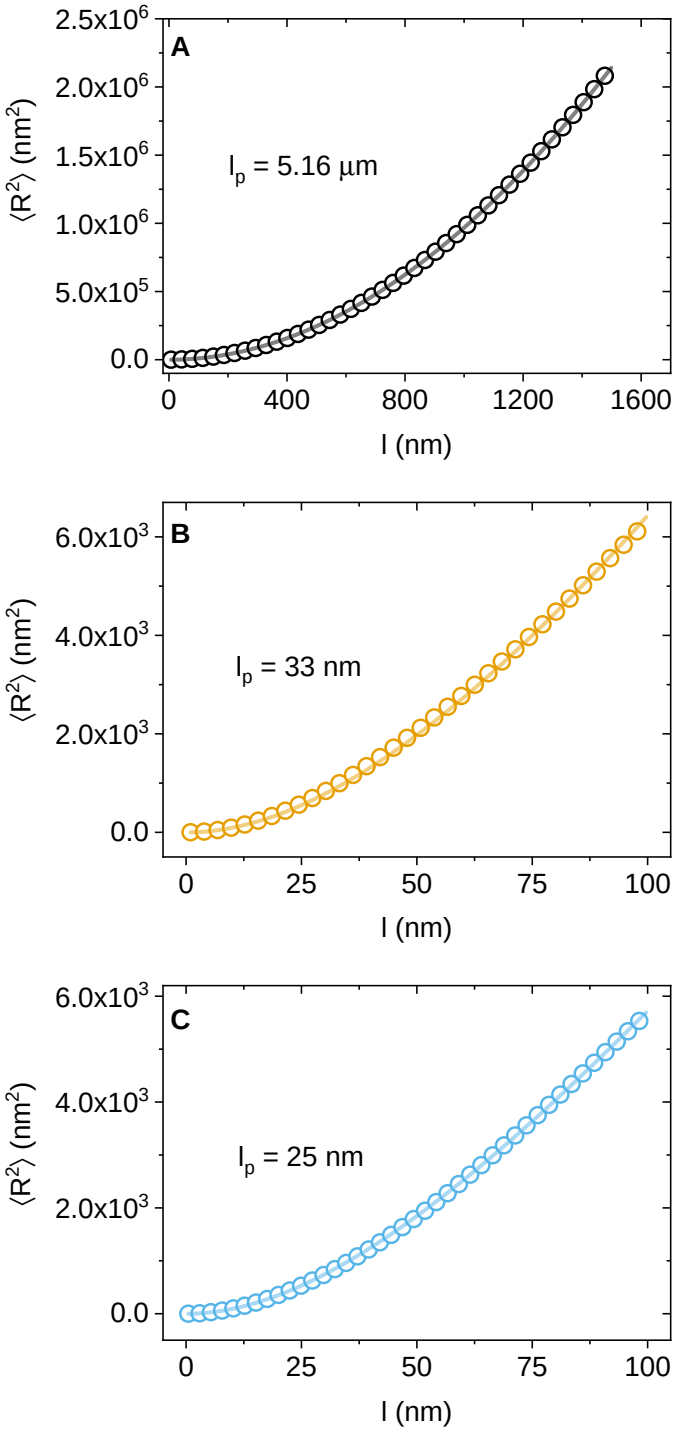

Fig. S2 Determination of the persistence length (l_p) of the analysed polymers (βLG amyloid fibrils, low-acetylated Gellan Gum and κ-carrageenan, in panels A, B and C, respectively), by fitting the mean-squared end-to-end distance ($\langle R^2 \rangle$) as a function of the internal contour length (l)[1]: $\langle R^2 \rangle = 4l_p[l - 2l_p(1 - \exp(-l/2l_p))]$. The obtained values are reported in Table 1 of the main manuscript.

3 Dissolution of κ-carrageenan and low-acetylated Gellan Gum at pH 2

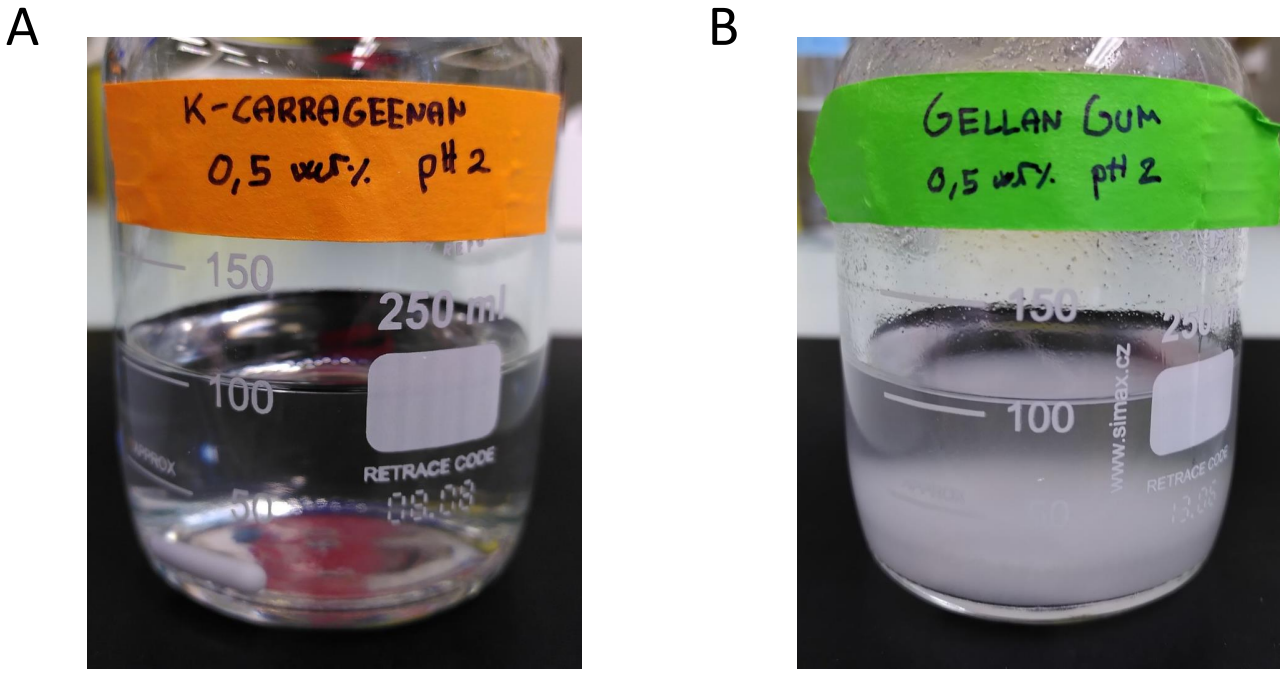

Fig. S3 Dissolution of κ-carrageenan (A) and low-acetylated Gellan Gum (B) at pH 2. The solutions were prepared by adding 0.5 g of the polysaccharides to 99.5 g of Milli-Q water at pH 2, followed by stirring for 1 h while heating at 90°C.

4 Rheological data - Loss tangent

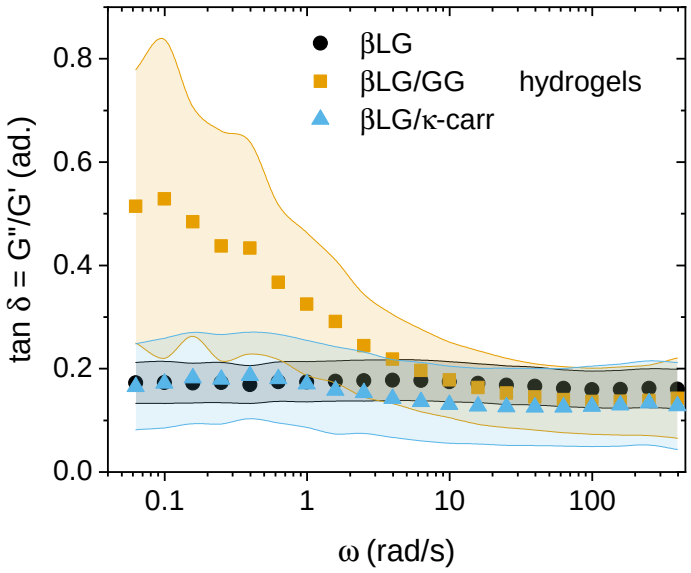

Fig. S4 Loss tangent ($\tan\delta = G''/G'$) calculated from the data reported in Fig.5A in the main manuscript. It can be appreciated how, while both βLG and βLG/κ-carrageenan networks exhibit average values smaller than 0.2, the values for the βLG/GG case raise to 0.5 (and are affected by larger error) as the probation frequency decreases. The error bars were computed using the formula $\sigma_\delta = (\sigma_{G'}/\langle G'\rangle + \sigma_{G''}/\langle G''\rangle)\cdot\langle\delta\rangle$

5 Compression experiments on hydrogels - Alternative normalization

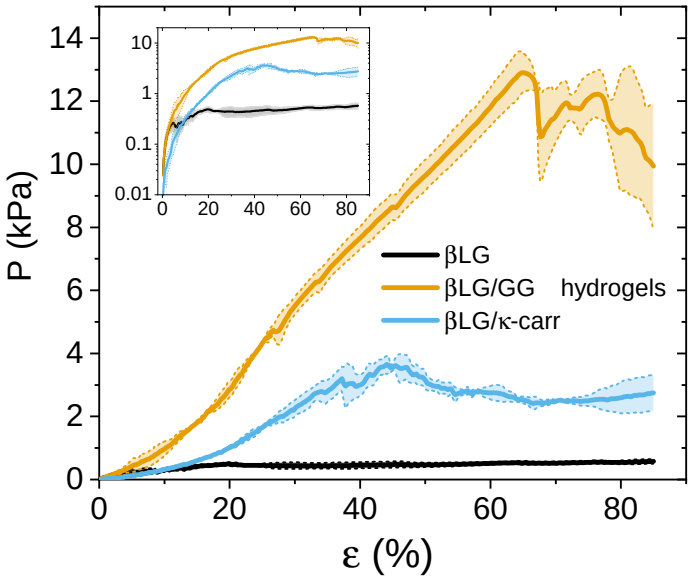

Fig. S5 Compression experiments on βLG amyloid fibril pure and hybrid hydrogels (in linear and semi-logharitmic scale, respectively in the main panel and in the inset). This figure was obtained similarly as Fig.5B and 5C of the main manuscript, but applying a different normalization that takes into account the incompressibility of water. In other words, as the upper plate of the geometry lowers and compresses the material, the effective cross-section of the sample is considered to increase to keep the total volume constant. If $V_0 = A_0 \cdot H_0$ is the initial volume of the gel, the assumption of the conservation of the entire volume leads to $A(t) = A_0 \cdot H_0/H(t)$, and the consequent real compression pressure is $P(t) = F(t)/A(t)$. Despite the reported pressure values are lower than the ones of the main manuscript (as a consequence of increasing compression area), the behaviour of the curves is similar and allows to draw the same conclusions on the relative compression properties of the examined materials.

6 Gold and methylene blue adsorption

6.1 Materials and methods

In order to characterize the ability of the synthesized gels for removing inorganic and organic pollutants from water, we decided to adsorb gold (in the form of $HAuCl_4$) and methylene blue as representative chemicals. For determining the adsorption capacity of the synthesized pure βLG and hybrid hydrogels, each of them was placed in contact with 4 mL of either a 2.5 mM solution of $HAuCl_4$ or a 2.5 ppm solution of methylene blue; the experiments were run over the course of 4 days, to allow the completion of the adsorption kinetics. Afterwards, the supernatants of the $HAuCl_4$ and the methylene blue solutions were sampled (1.5 mL and 2 mL, respectively) and analysed by AAS (Atomic Adsorption Spectroscopy) and UV-Vis Spectroscopy. The experiments were performed in triplicates, for each gel type, and the results were compared with those obtained from solutions where no gels were immersed. In the case of pure Gellan Gum gels (used as a control for determining the adsorption capacity of the polysaccharide unit), the gel was left immersed in a $\sim$ 70 ppm $HAuCl_4$ solutions (in duplicate, 4 mL each), and the experiment was then conducted as described above (after the system reached saturation). The pure Gellan Gum gels were prepared following the same protocol as the pure βLG amyloid fibril gels, with the difference that their formation was driven by immersing the cut syringe in a 100 mM KCl solution at pH 7, without further pH adjustment steps.

6.2 βLG amyloid fibrils preserve their surface functionality

In previous studies, it was shown that amyloids have a high binding capacity for heavy metal ions and organic pollutants[2–4], and therefore, show a significant potential for universal water purification. The way the polysaccharide fraction is embedded in the final hybrid materials can be deduced from the adsorption efficiency of the composite materials: if the protein-polysaccharide hydrogels show similar adsorption performances as the pure βLG networks, and if the polysaccharides do not play an active role in adsorbing the pollutants, then it is likely that the carbohydrate fraction forms an independent network (or local bundles). On the other hand, if the adsorption performance of the βLG component is

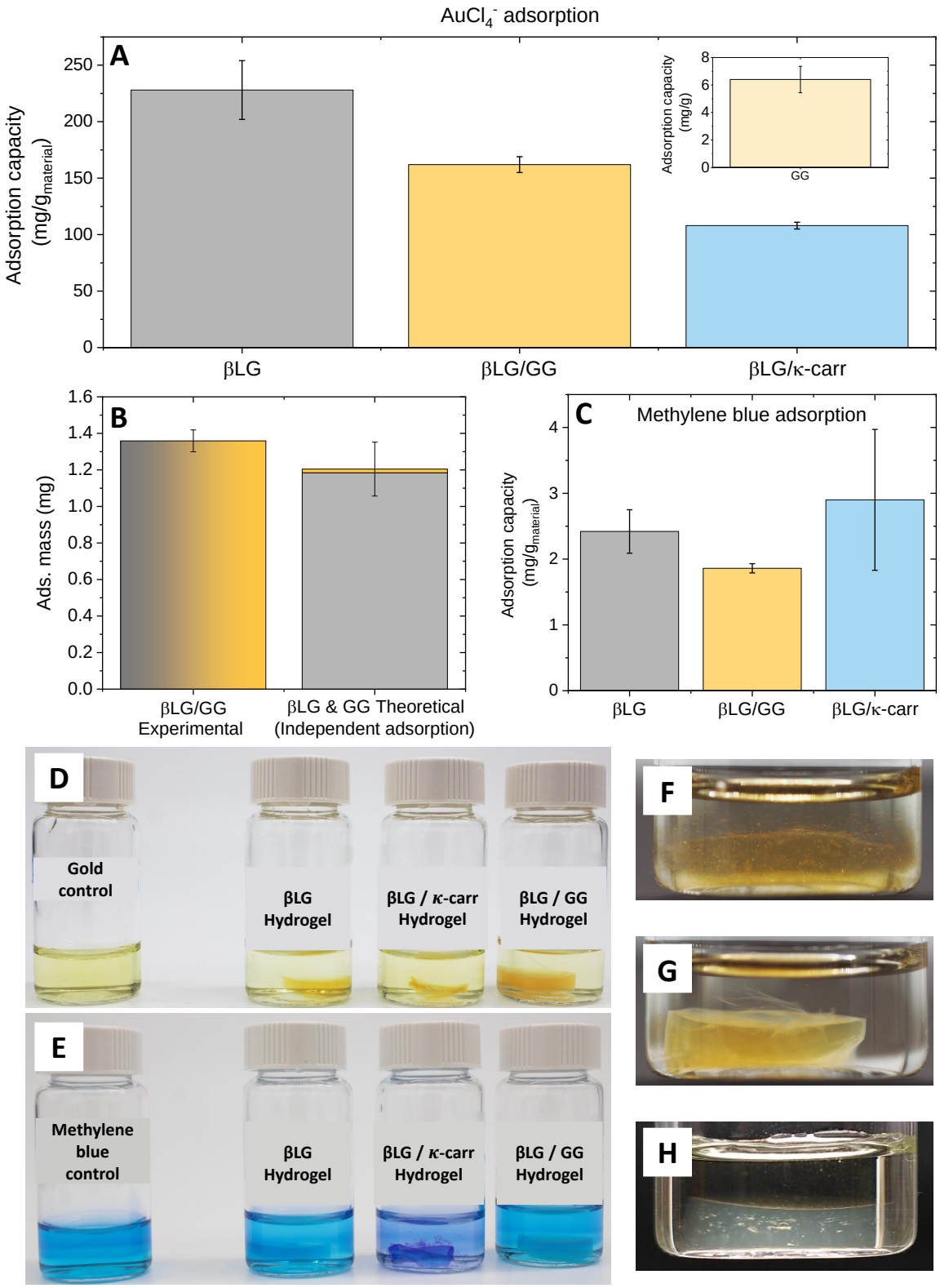

Fig. S6 Adsorption of the synthesised pure βLG amyloid fibril hydrogels and hybrid ones towards a gold salt ($HAuCl_4$) or of an organic pollutant (methylene blue). (A) Adsorption capacity of the three systems towards the gold salt. Inset: Adsorption capacity of a pure Gellan Gum gel towards the same chemical specie. (B) Comparison between the experimentally measured adsorbed mass (of the gold salt) by the hybrid βLG/GG gels, and the theoretical adsorbed mass of a fictitious material (built up by the identical masses of the protein and polysaccharide), where an independent action of the two components is assumed. (C) Adsorption capacity of the three systems towards methylene blue. The results for the βLG/κ-carrageenan case are affected by specific interactions that modify the visible light absorption spectrum of the considered dye. (D) Visual inspection on the ability of the gels to adsorb $HAuCl_4$. (E) Visual inspection on the ability of the gels to adsorb an organic dye (methylene blue). (F-G) Closer look on a pure βLG amyloid fibril gel (F) and a βLG/GG hybrid gel (G) immersed in a $HAuCl_4$ solution. (E) Picture of a pure Gellan Gum gel immersed in a $HAuCl_4$ solution.

severely hindered, and the sugar units show limited binding capacities, it is instead likely that the polysaccharide units cover the fibrils and prevent them from interacting with the pollutants.

Fig.S6A shows the adsorption capacities of the pure amyloid fibril and hybrid gels towards gold (in an anionic form, $AuCl_4^-$). While the pure βLG samples show an average value higher than 225 mg/g, the hybrid materials show lower performances (approximately 160 and 120 mg/g for the βLG/GG and the βLG/κ-carrageenan gels, respectively). Although this may be interpreted as a hint that the polysaccharide fraction inhibits the adsorption of the pollutant, we need to consider that the adsorption capacity is calculated by dividing the adsorbed quantities by the masses of the adsorbing materials (that we considered equivalent to the average dry masses reported in Fig.3C of the main manuscript). Therefore, as the normalization is performed by also considering the masses of the polysaccharide fractions (that we hypothesize to play a small role in the adsorption), the data do not reflect the real adsorption capacity of the protein. Before proceeding with the analysis, we verified the accuracy of this hypothesis, by determining the adsorption capacity of Gellan Gum (inset of Fig.S6A). While all the gels containing the protein fraction are characterised by values higher than 100 mg/g, the pure polysaccharide system shows much poorer performances (close to 6 mg/g). Thus, our hypothesis that Gellan Gum plays a marginal role in the examined adsorption phenomena is verified.

This analysis leads to Fig.S6B, where the experimentally measured performance of the βLG/GG hydrogels (in terms of adsorbed mass) is compared to the theoretically-determined performance of a system where the same average quantities of βLG amyloid fibrils and Gellan Gum act independently. To do so, we considered that the hybrid materials have an average dry mass of 8.4 mg, 5.2 mg of which can be assumed to be the βLG amyloid fibrils and the difference (3.2 mg) to be the polysaccharide fraction (Fig.3C in the main manuscript). An ideal hybrid material, constituted by protein and polysaccharide components that act independently, would adsorb the same quantity of pollutants as the pure βLG amyloid fibril gels (gray bar), plus the quantity that can be ascribed to the polysaccharide fraction (ochre bar), determined by multiplying the measured adsorption capacity of Gellan Gum (inset of Fig.S6A) by the mass of the just-mentioned polysaccharide component. The result is very interesting: the average experimental adsorbed quantity from the hybrid system (bar with gray/ochre gradient) is in close agreement with the theoretically determined one. Therefore, it can be stated that the presence of Gellan Gum does not alter the adsorption capacity of the amyloid fibril fraction. However, the same scenario might not be true for the κ-carrageenan case: in fact, both the total dry mass (Fig.3C in the main manuscript) and the adsorption capacity are lower when compared to the other hybrid network. The reduced adsorption capacity might be ascribed to the shrinkage observed in this system (which reduces the specific surface area), and not resulting instead from specific interactions between the proteins and the considered sulfated polysaccharide fraction.

A visual inspection of the adsorption performances of the analyzed materials towards the used gold salt is shown in Fig.S6D, F, G and H, that report preliminary experiments with gold solution whose concentration was higher than the adsorption capacity of the materials. In panel D, it is possible to clearly appreciate how the color of the gels is darker than the one of the surrounding solution, clearly stating the ability of the considered materials to adsorb gold. Panels F and G show a closer look to pure βLG and βLG/GG hybrid gels, respectively, after they were left immersed in a gold solution for many days. In the case of the pure protein sample, the gold is transformed from its ionic form to its metallic counterpart, with creation of gold crystals[5] (visible as golden fragments that get released). Such release phenomenon is not visible in the hybrid gel case, potentially as a consequence of the stronger nature of the network: we believe this being an advantage of the mentioned hybrid material over the pure protein one, as it would less likely re-pollute the treated water in real-life applications. Panel H shows, instead, a pure Gellan Gum gel immerse in a gold solution. The image was acquired with a dark background to show the extremely limited adsorption capacity of the mentioned polysaccharide towards the considered ionic species. In fact, there is not hint of gold-like colour inside the gel mesh.

We extended the adsorption analysis further, including a dye (methylene blue) as a representative of organic pollutants. From Fig.S6B, it can be seen again how the hybrid systems show a performance similar to the pure βLG amyloid fibril networks. However, the performance of the βLG/κ-carrageenan hybrid system appears to be superior (despite the significant experimental error), in contrast to what was observed for gold adsorption. Considering the appearance of the gels after adsorption in preliminary trial experiments (Fig.S6E), where the used methylene blue concentration was much higher than the adsorption capacity of the material, we can clearly state that this result is caused by modifications in the optical absorption properties of the dye. In fact, the different color of the final system from that of the control solution (purple instead of blue) is a benchmark of specific interactions between the gel and the dye[6], or of pH induced structural changes of methylene blue[7] (in fact, βLG/κ-carrageenan hybrid gels were formed at a slightly higher pH than the others, to lower shrinkage effects). Therefore, we believe that the higher adsorption capacity observed in this case is an artifact

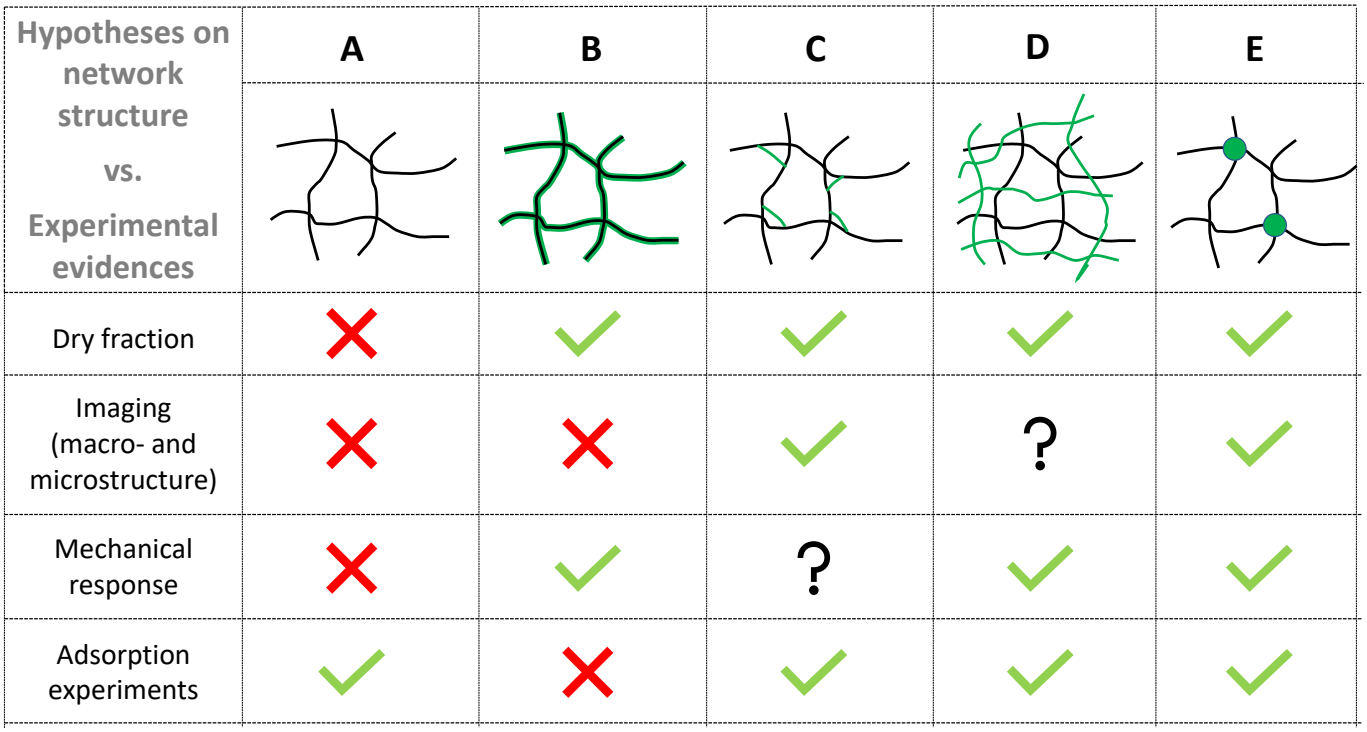

Fig. S7 Analysis on how different embedding models of the polysaccharides inside the βLG amyloid fibril network align with the results of the performed experiments. (A) Pure amyloid network, where no polysaccharides could diffuse in. (B) Core-shell structure, with the protein fraction surrounded by the diffused polysaccharides. (C) Cross-linked network, where the polysaccharides interact with the amyloid fibrils and, without coating behaviour, strengthen the interactions among them. (D) Interpenetrating network, where the polysaccharide fraction builds up a secondary network that exists in parallel to the amyloid one. (E) Local bundling, where the polysaccharides concentrate in specific parts of the network and strengthen it with the formation of local thicker strands. In the discussion, the different hypothesis are compared with the results of the performed experiments.

induced by such phenomena. For methylene blue, we did not attempt to evaluate the adsorption performance of the pure polysaccharide fraction separately, as the adsorption performance of amyloid fibrils towards this dye is lower compared to gold. As a consequence, it would have been more complex to clearly identify the contributes of the protein and of the polysaccharide fractions.

To conclude, the experimental evidence presented here suggests that, apart from shrinkage-induced surface area reduction, the presence of the polysaccharide (especially in the Gellan Gum case) does not alter the adsorption performances of the amyloid fibrils. This is a key piece of information that suggests a good degree of preservation of the surface reactivity of amyloid fibrils.

7 Hypotheses on network structure

In our analysis on the synthesised pure protein and hybrid hydrogels and aerogels, carried our in the main manuscript and enriched by further insights presented here, we showed an effective diffusion of the sugar chains inside the networks (confirmed by the increase in the dry fraction of the final materials). Then, by analysing the macro- and microscopic appearance of the materials, by probing their mechanical properties through oscillatory sweeps and compression experiments, and by studying their performances in adsorbing water pollutants, we gained further insights on their structure and performances. While the higher compressibility and the remarkable adsorption capacity of the hybrid materials were confirmed by the performed experiments, the individual characterizations did not allow to draw conclusions on the microstructure of the arrested fibrillar networks. In fact, in the SEM images (Fig.4G, H and I in the main manuscript) the polysaccharide component could not be identified in a straightforward way: the presence of bundles in the aerogels could be interpreted both as characteristic interactions between the two components, or as shrinkage-induced lateral aggregation of filaments. Therefore, to draw stronger conclusions on how the polysaccharides are present in the final hybrid gels and aerogels, we compare all the collected evidence against different hypotheses (Fig.S7). A first hypothesis (A) consists in assuming that, due to repulsive charges and steric hindrance, the polysaccharide do not effectively diffuse inside the amy-

loid mesh. As such hypothesis is contradicted by the dry fraction analysis, by the performed imaging and by the measured mechanical reinforcement, it can be rejected. A second hypothesis (B) assumes that the polysaccharides, upon diffusion inside the amyloid fibril mesh and after getting in touch with the gelling salt solution, cover the amyloid fibrils and create a core-shell network. While this hypothesis is potentially aligned with the dry fraction measurements and the mechanical characterization (where the increased resistance to compression could be interpreted as an increase in bending stiffness of single filaments), the results from the imaging characterisation and from the adsorption measurements contradict such scenario. In fact, in the SEM images it is possible to appreciate only local hints of aggregation, and in the adsorption of the gold salt and of methylene blue the amyloid network almost fully express its surface reactivity. We believe therefore that it is safe to reject this second hypothesis.
A third scenario (C) consists in assuming that the diffused polysaccharide units interact with the fibril network by the creation of local cross-links. While such structure could be aligned with almost all the described evidences, we are skeptical of it being able to explain the observed mechanical response. In fact, upon diffusion of ions, amyloid fibrils create long-lived physical crosslinks that strongly tune their rheological response[8]: while it is possible that crosslinking with the polysaccharide units further reinforces the networks, it is doubtful that the mentioned process could strengthen the materials to the observed extent. The forth hypothesis (D) we consider consists in the polysaccharide chains being morphologically affected by the added specific ions, and creating therefore a secondary network that interpenetrates the amyloid fibrils one. This hypothesis is aligned with the dry fraction analysis, with the observed increase in mechanical properties and with the adsorption characterization; at the same time, the SEM images presented in the main manuscript do not show a network which is appreciably denser for the hybrid aerogel cases. In fact, the presence of a secondary network is not the most straightforward interpretation of the mentioned pictures; however, it could also be assumed that a secondary network was present before the CO_2 drying process, and then collapsed and reinforced the primary network over the solvent exchange (this phenomenon is confirmed by the fact that polysaccharide aerogels, at the mass fraction values compatible to the ones of our work, usually shrink a lot). The last hypothesis that we share (E) is that the polysaccharide component, upon diffusion and ion-induced morphological modifications, forms local bundles that strengthen the βLG network by locally increasing the bending stiffness. This hypothesis is not contradicted by the collected experimental evidence and, together with the hypotheses (C) and (D), builds different pathways that could explain the properties of the observed networks. The hypothesis that the hybrid materials consist in double network gels (DN) is not considered, as such materials are usually built by combining a rigid and brittle cross-linked polyelectrolite network, together with a neutral, soft and ductile polymer present at much higher molarity[9,10].

References

1 I. Usov and R. Mezzenga, *Macromolecules*, 2015, **48**, 1269–1280.

2 S. Bolisetty and R. Mezzenga, *Nature Nanotechnol.*, 2016, **11**, 365–371.

3 M. Peydayesh, S. Bolisetty, T. Mohammadi and R. Mezzenga, *Langmuir*, 2019, **35**, 4161–4170.

4 M. Peydayesh, M. K. Suter, S. Bolisetty, S. Boulos, S. Handschin, L. Nyström and R. Mezzenga, *Adv. Mater.*, 2020, **32**, 1907932.

5 G. Nyström, M. P. Fernández-Ronco, S. Bolisetty, M. Mazzotti and R. Mezzenga, *Adv. Mater.*, 2016, **28**, 472–478.

6 M. Diener, J. Adamcik and R. Mezzenga, *ACS Macro Lett.*, 2020, **9**, 1310–1317.

7 G. Singhal and E. Rabinowitch, *J. Phys. Chem.*, 1967, **71**, 3347–3349.

8 Y. Cao, S. Bolisetty, J. Adamcik and R. Mezzenga, *Phys. Rev. Lett.*, 2018, **120**, 158103.

9 J. P. Gong, *Soft Matter*, 2010, **6**, 2583–2590.

10 Q. Chen, H. Chen, L. Zhu and J. Zheng, *J. Mater. Chem. B*, 2015, **3**, 3654–3676.